Journal of the European Ceramic Society **10** (1992) 115–122

The Effects of Sintering Atmosphere on Impurity Phase Formation and Grain Boundary Resistivity in Y_2O_3-Fully Stabilized ZrO_2

S. P. S. Badwal & A. E. Hughes

CSIRO, Division of Materials Science and Technology, Locked Bag 33, Normanby Road, Clayton 3168, Victoria, Australia

(Received 2 September 1991; accepted 6 November 1991)

Abstract

X-ray photoelectron spectroscopy and impedance studies have been used to monitor the migration of the impurity silicate phase in the grain boundary network of fully stabilized Y_2O_3–ZrO_2 sintered at different temperatures in air. The nature of the grain boundary phase formed and its influence on the grain boundary resistivity were considerably different under air compared with the previously reported argon-sintered specimens. As a function of the sintering temperature, two peaks were observed in the XPS atomic ratios (Y/Zr, Si/Zr, O/Zr) at the fractured surfaces of air-sintered specimens, while in argon-sintered specimens only one peak was present. There is a high degree of correlation between the grain boundary resistivity and XPS atomic ratios. The activation energy for the grain boundary resistivity is independent of the sintering temperature and atmosphere and is similar to that for the lattice resistivity. No evidence was found for perfect wetting of grains by the impurity glass phase at any sintering temperature. Instead, the results strongly support a discontinuous grain boundary phase model.

Es wurden Röntgen-Photoelektron-Spektroskopie und Impedanz-Messungen herangezogen, um die Wanderung der Silikat-Verunreinigungsphase im Korngrenzennetzwerk von vollständig stabilisiertem Y_2O_3–ZrO_2, welches bei verschiedenen Temperaturen an Luft gesintert wurde, zu verfolgen. Die Art der gebildeten Korngrenzenphase und deren Einfluß auf den Korngrenzenwiderstand sind deutlich unterschiedlich für an Luft gesinterte Proben und für in Argon-Atmosphäre gesinterte Proben, über die vorher berichtet wurde. In Abhängigkeit der Sintertemperatur konnten in den XPS Atomverhältnissen (Y/Zr, Si/Zr, O/Zr) zwei Peaks an den Bruchoberflächen Luft-gesinterter Proben beobachtet werden, während bei Argon-gesinterten Proben nur ein Peak beobachtet wurde. Der Korngrenzenwiderstand und das XPS Atomverhältnis sind in hohem Maße miteinander korreliert. Die Aktivierungsenergie des Korngrenzenwiderstandes ist sowohl von der Sintertemperatur als auch von der Sinteratmosphäre unabhängig und ähnelt der des Gitterwiderstandes. Bei keiner Sintertemperatur konnte eine vollständige Benetzung der Körner durch die Verunreinigungsphase beobachtet werden. Die Ergebnisse stützen dagegen vielmehr ein Modell mit diskontinuierlicher Korngrenzenphase.

La spectroscopie photoélectronique de rayon X et des études d'impédance ont été utilisées pour suivre la migration de la silice sous forme d'impureté dans le réseau de joints de grains de Y_2O_3–ZrO_2 complètement stabilisé et fritté à l'air sous différentes températures. La nature de la phase de joint de grains formée et son influence sur la résistance des joints de grains ont été considérablement différentes à l'air en comparaison avec les échantillons frittés sous argon de la publication précédente. Deux piques ont été observés dans les rapports atomiques XPS (Y/Zr, Si/Zr, O/Zr) en fonction de la température de frittage au niveaux des surfaces fissurées des échantillons frittés à l'air, alors que les échantillons frittés sous argon ne présentaient qu'un seul pique. Il existe un haut degrés de corrélation entre la résistance des joints de grains et les rapports atomiques XPS. L'énergie d'activation pour la résistance des joints de grains est indépendante de la température de frittage et de l'atmosphère, et est semblable à celle de la résistance

du réseau. Aucune preuve n'a été trouvée d'un recouvrement parfait des grains par la phase amorphe qui est présente sous forme d'impureté quelque soit la température de frittage. Au contraire les résultats sont plutôt en faveur d'un modèle de phase discontinue aux joints de grains.

1 Introduction

The presence of grain boundary impurity phases in yttria–zirconia ceramics can have a marked affect on the oxygen ion conducting properties of the material. Studies of the effect of sintering atmosphere on the nature of the grain boundary impurity phase have been undertaken. For example, in a previous study on Ar-sintered yttria-fully stabilized zirconia (Y-FSZ) it was found that an inflection in the grain boundary resistivity, as measured by impedance dispersion analysis, was related to the morphology of the grain boundary impurity phase.[1] Specifically, after sintering in Ar at 1300°C, there was a considerable wetting of the grain boundary network by an impurity silicate phase. Above 1500°C the grain boundary network was relatively clean and a considerable amount of the impurity silicate had migrated to the external surface. The correlation between the morphology of the impurity phase and the grain boundary resistivity was established by X-ray photoelectron spectroscopy (XPS)[2] and transmission electron microscopy (TEM).[3]

In an earlier study[4] preliminary results suggested that the nature of the silicate grain boundary phase formed in specimens sintered in air was different to that formed in argon. In this paper, by using impedance dispersion analysis, XPS and scanning electron microscopy, the authors have intensively examined the characteristics of the impurity phases formed in air-sintered Y_2O_3-fully stabilized ZrO_2 (Y-FSZ). Comparison of the results with the Ar-sintered material reveals that the sintering atmosphere plays just as important a role as the impurity profile of the starting powder in effecting the grain boundary resistivity.

2 Experimental Procedure

The high-purity, fine-grain prereacted powder, designated YSZ10V, with a composition of 10 mol% Y_2O_3 + 90 mol% ZrO_2 quoted by the manufacturer (Viking Chemicals Ltd, Denmark) was pressed into disks in a 12·5 mm die and sintered in air at temperatures ranging from 1300°C to 1700°C. The heating rate was 300°C h^{-1} and samples were held at the target temperature for 15 h and then cooled at 300°C h^{-1}.[2] Some specimens were also prepared in an argon atmosphere (oxygen concentration in the vicinity of 10 ppm), again, under identical conditions to the air-sintered disks, for direct comparison of the data. The analysis of impurities in the starting powder has been given elsewhere by Badwal & Drennan.[3] The SiO_2 content was in the vicinity of 20–60 ppm. No attempt was made to analyse the powder for the yttrium content. Densities were measured from specimen dimensions and weight.

Intergranular fracture surfaces were generated by thermal downshock; samples were rapidly quenched from 1000 to −196°C (liquid nitrogen). As determined by SEM, this method usually generated around 60% intergranular fracture, although in some cases as low as 40% was observed. Figure 1 displays the fracture surface of samples sintered at 1350, 1500 and 1600°C. The total grain boundary surface area decreased with increased sintering temperature as a result of grain growth. The ratio of intragranular to the total grain boundary surface area obtained was only slightly affected by the sintering temperature. All the XPS results presented were averaged over several fracture surfaces and error bars take account of the variable amount of intergranular fracture.

For XPS analysis samples were mounted with

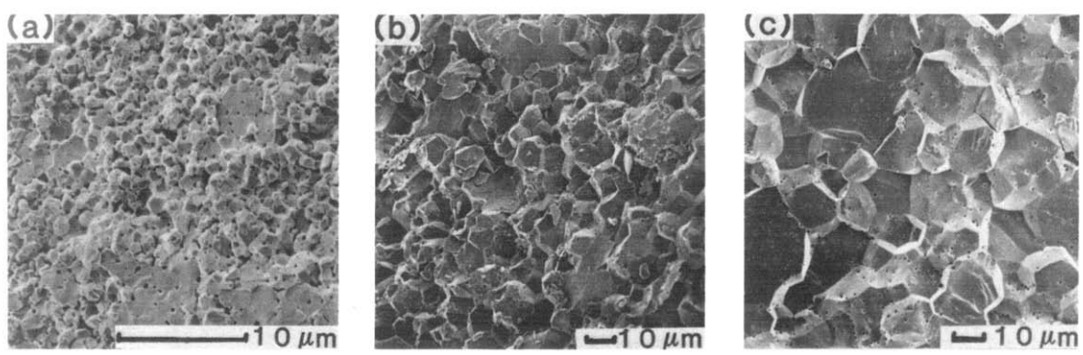

Fig. 1. Scanning electron micrographs of the fracture surface of specimens sintered in air at (a) 1350°C, (b) 1500°C and (c) 1600°C.

either double-sided adhesive tape or held in a metal spring-loaded clamp, spot welded to the top of the sample stub. The treatment of the data has previously been described and will only briefly be considered here.[2] The Zr 3*d* 5/2 line (182·2 eV) was used as a reference peak to correct for sample charging. XPS atomic ratios were calculated by the normal procedure.[2] Curve fitting was employed to estimate the Y 3*d* intensity, since there was overlap between the Y 3*d* and Si 2*s* photoelectron peaks.

Impedance measurements were made on sintered disks (2·0–2·8 mm thick with a diameter of 9·3–9·7 mm) between 280 and 400°C and over the frequency range of 5–10 MHz with a HP 4192LF impedance analyser interfaced to a desk-top computer. For these measurements YSZ10V disks were ground flat before the application of the Pt electrode paste.

3 Results

The densities of the specimens sintered in air were generally slightly lower than those sintered in an argon atmosphere (Table 1). The XPS atomic ratios for Y/Zr, Si/Zr, O/Zr and Na/Zr measured on the external surface of specimens are displayed in Fig. 2 as a function of the sintering temperature. The Y/Zr ratio displayed a peak with a maximum of 0·35 at 1300°C, then decreased in a stepwise fashion to 0·30 at 1700°C. The Si/Zr and Na/Zr ratios both displayed maxima in their temperature dependence at 1450 and 1350°C respectively, but at sintering temperatures in excess of 1500°C were nearly constant. The O/Zr ratio increased with increasing sintering temperature and displayed a broad peak centred at ≈1550°C.

For the fracture surface (Fig. 3) of air-sintered specimens, the Y/Zr, Si/Zr and O/Zr ratios all displayed similar behaviour, exhibiting two peaks as a function of the sintering temperature, as opposed to only one peak reported for argon-sintered disks.[1,2] The Y/Zr ratio increased from a value of 0·30 at 1200°C to a maximum of around 0·35 at 1300°C, then decreased to about 0·29 between 1350

Table 1. The measured densities of sintered ceramics and activation energy values for grain boundary and lattice resistivities as a function of the sintering temperature and gas atmosphere

Sintering temperature (°C)	*Density* (% *theoretical*)		*Activation energy* ($kJ\,mol^{-1}$ (±3))			
	Air	*Argon*	*Grain boundary*		*Lattice*	
			Air	*Argon*	*Air*	*Argon*
1300	92·5	92	114	112		
1400	96	97	113	115	113	115
1500	96·5	98	109	113		
1600	97	98	111	116	112	117
1700	97	98	109	116		

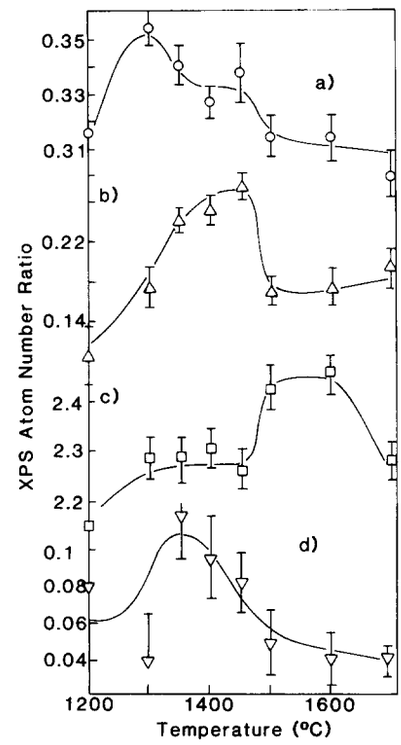

Fig. 2. XPS atomic ratios for the external surface of specimens (air-sintered) as a function of the sintering temperature. (a) Y/Zr, (b) Si/Zr, (c) O/Zr and (d) Na/Zr.

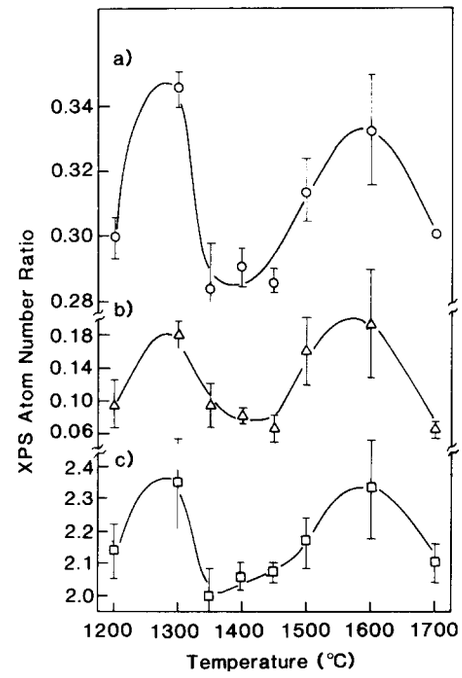

Fig. 3. XPS atomic ratios for the fracture surface of specimens (air-sintered) as a function of the sintering temperature. (a) Y/Zr, (b) Si/Zr and (c) O/Zr.

and 1450°C. Above 1450°C it increased again to a second maximum of 0·33 at 1600°C, then decreased to 0·30 at 1700°C. The temperature dependencies of the Si/Zr and O/Zr ratios were similar to that of the Y/Zr ratio. Peak maxima were observed for the Si/Zr and O/Zr ratios between 1200 and 1300°C of 0·18 and 2·36, respectively, and maxima at 1600°C of 0·19 and 2·33, respectively. Sodium was always present at the fractured surface but the Na/Zr ratio displayed only random variation with the sintering temperature.

The spectroscopy results for the external and fracture surfaces are plotted on a two-dimensional chemical state plot for silicon in Fig. 4.[5] Reference compounds included on the plot are the silicas, quartz (Q) and aerosil (A), and $Y_2(SiO_4)O$—yttrium orthosilicate (X). The region labelled Ar represents the results obtained for the impurity silicate at the fracture and external surfaces of the Ar-fired specimens presented previously.[2] The diagonal lines on the two-dimensional chemical state plot are lines of constant Auger parameter, α', and essentially represent similar ability of neighbouring atoms, in this case oxygen atoms, to screen final state ions. The ability of the surrounding oxygens to provide electron density to screen the final state ion reflects, in a crude way, the structure of the material. Hence the value of α' is an indicator of the intermediate-range order in the material.

The results for the fracture and external surface of the air-fired YSZ10V showed a large amount of scatter, although they may be broadly divided into two groups. One group approximately coincides with the results for the Ar-fired surface. These results are typical of glassy silicate phases. The second group, labelled U, have a much larger α' parameter and higher Si (KLL) kinetic energy ($\geq$1611·0 eV). Group U corresponds to the data measured on the fractured surface for specimens sintered between 1350 and 1500°C. It is not clear what physical interpretation should be given to the high α' values. Glassy phases generally have α' values between 1712 and 1712·8 eV.[6] There is evidence,[4] however, to suggest that the crystalline phase can have an α' value up to 1 eV higher than the glassy phase. Hence the group labelled U in Fig. 4 may well be related to the crystallization, on cooling, of the glassy phase that remained in the grain boundary network.

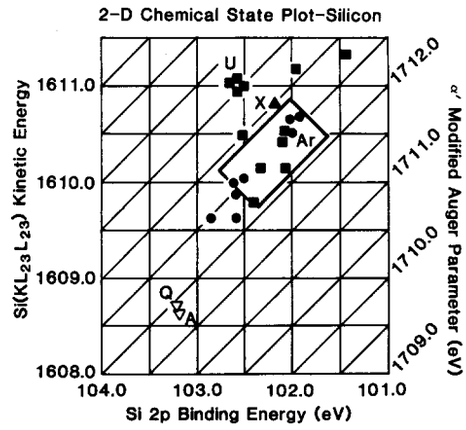

Fig. 4. Silicon two-dimensional chemical state plot for XPS data obtained on the fracture (■) and external (●) surfaces of specimens sintered in air at various temperatures.

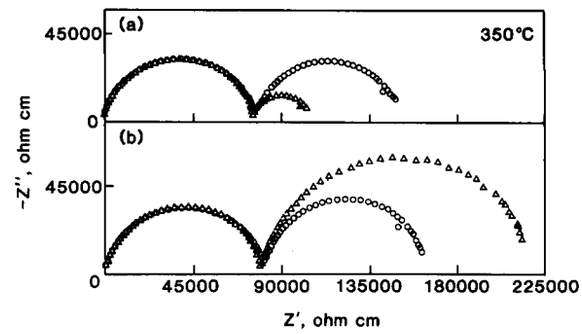

Fig. 5. Impedance spectra recorded at 350°C of specimens sintered in (a) argon and (b) air at (○) 1400°C and (△) 1600°C.

Figure 5 shows the impedance spectra for specimens sintered at 1400°C and 1600°C in both air and argon atmospheres. At 1600°C, the grain boundary resistivity was higher for air- and lower for argon-sintered specimens compared with the respective disks sintered at 1400°C. The lattice resistivity, R_l, as expected, was independent of the sintering temperature or the gas atmosphere once the specimens had achieved near theoretical density (Fig. 6). Minor differences observed in Figs 5 and 6 can be accounted for by the slightly different densities of disks sintered in different atmospheres, especially at the lower sintering temperature. Figure 7 shows a plot of the grain boundary resistivity versus sintering temperature for both air- and argon-sintered specimens. The measured grain boundary resistivity, R_{gb}, in zirconia-based electro-

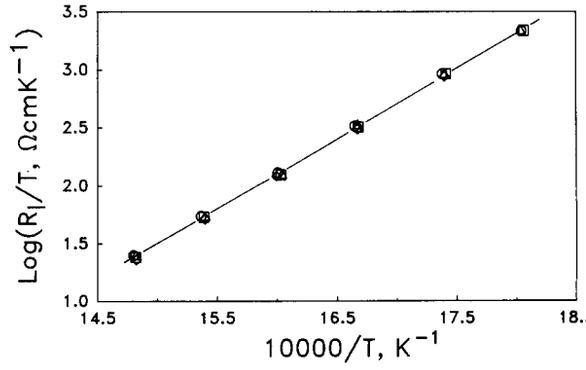

Fig. 6. Arrhenius plots for the lattice resistivity of specimens sintered at 1400°C (○□) and 1600°C (△◇) in air (○△) and (□◇) argon atmospheres.

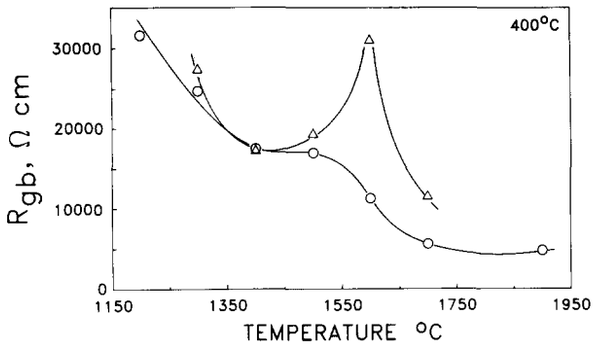

Fig. 7. Plots of the grain boundary resistivity data recorded at 400°C versus the sintering temperature. (○) Argon and (△) air.

lytes, in general, decreases with increasing sintering temperature. This indeed was the case for argon-sintered specimens except for the appearance of an inflection at around 1400°C. However, R_{gb} for air-sintered disks firstly decreased on going from a sintering temperature of 1300°C to 1400°C and then it increased with further increase in the sintering temperature up to 1600°C (Fig. 7). Above 1600°C, a decrease in the grain boundary resistivity was observed. These results are in sharp contrast to those obtained for argon-sintered specimens but consistent with the XPS data. The activation energy for the grain boundary resistivity was independent of the gas atmosphere or the sintering temperature (Table 1).

4 Discussion

The major difference between air- and argon-sintered specimens is that the Si/Zr and Y/Zr atomic ratios at the fractured surfaces, plotted as a function of the sintering temperature, exhibited two peaks for air-sintered disks (Fig. 3) and only one peak for argon-sintered specimens.[1,2] The second peak in the atomic ratios, for air-sintered specimens, corresponds to the peak in the grain boundary resistivity versus sintering temperature curve. The XPS data, combined with impedance results, clearly indicate that there is a considerable redispersion of the impurity phase as a function of the sintering temperature. For argon-sintered specimens, the inflection around 1400°C in the plot of grain boundary resistivity versus sintering temperature corresponded with the only peak observed in the XPS atomic ratios (Si/Zr, Na/Zr, Y/Zr).[2,3] Furthermore, it was evident from increases in the atomic ratios on the external surface that the impurity phase had migrated to the exterior of the specimens at and above 1500°C. As with the Ar-sintered results presented previously,[2,3] the dependence of the atomic number ratios for the air-sintered specimens can also be interpreted in terms of redispersion of impurity material in the grain boundary network and migration to the external surfaces. For example, peaks in the sintering temperature dependence of the atomic ratios on the fracture surface are probably a combination of loss of surface area due not only to grain growth but, more importantly, also to a more homogeneous spreading of the material throughout the grain interface (see later). The impurity phase is more sensitive to detection by XPS when it is spread as a thin film over the grain boundary, hence peaks in the temperature dependence of the atomic ratios are associated with changes in impurity phase morphology.

Providing an explanation for the observed trends in the XPS and impedance data is difficult, due to the complex nature of the system under study. In the following section the authors have attempted to devise a model which is consistent with the observed trends and which may provide a starting point for understanding segregation phenomena in such systems.

For air-sintered disks, sintering starts between 1200 and 1300°C, and at 1300°C the ceramic attains reasonably high density (Table 1). The wetting of the grain boundary network by the impurity silicate phase appears to accompany densification of the ceramic. This is evident from increases in the XPS atomic ratios (especially Si/Zr and Y/Zr) and a high value for the grain boundary resistivity.

Between 1350 and 1450°C, in the XPS data, the atomic ratios associated with the impurity phase are considerably less and the grain boundary resistivity much lower than at 1300°C. Normally, for a constant amount of the grain boundary phase in the bulk, the XPS atomic ratios at the fractured surface arising from an impurity phase (glassy phase component/Zr) would be expected to increase with the sintering temperature. This increase results from a given amount of the impurity phase being spread over an ever-diminishing grain boundary surface area (due to grain growth) assuming that it stays within the ceramic as a thin layer surrounding almost all grains. For the air-sintered specimens, the trend is the opposite; the Si/Zr and Y/Zr ratios decrease from 1300 to 1350°C and then remain almost constant up to 1450°C despite considerable grain growth and resulting decrease in the grain boundary surface area. This behaviour stems from a change in the morphology/composition of the grain boundary phase, possibly from less wetting of the grain boundary network and/or migration of some impurity phase to the external surface. There is

sufficient evidence from this work that a sodium-rich silicate phase migrates to the external surface for sintering temperatures between 1350 and 1450°C (Na/Zr and Si/Zr display maxima in Fig. 2). Clearly, however, there is still some silicate resident in the grain boundary network, since the Si/Zr ratio is not zero at the fractured surface. Furthermore, the silicate phase present in the grain boundary network (between 1350 and 1450°C) is different to that present on the fractured surface at 1200 and 1300°C or to the Na-rich silicate on the external surface, since its spectroscopic values (group U in Fig. 4) are different. Thus for air-sintered specimens it appears that the silicate which is formed in the grain boundary network between 1200 and 1300°C either does not form at higher temperatures or else decomposes above 1300°C to a number of different silicates. Some evidence for the latter exists from a separate study on the stability of Na–Y–silicate phases in different gas atmospheres.[7] In this study an amorphous $Na_3YSi_2O_7$ was heated at 1500°C in either air or argon atmospheres and specimens characterized by XRD, NMR and chemical analysis both before and after the heat treatment. Loss of sodium was observed, due to heat treatment in both air and argon, leading to yttrium enrichment of the silicate. In one experiment the phase remained amorphous in nature when heat treated in an argon atmosphere (fast gas flow rate), while in air considerable crystallization occurred. In the second experiment with slow argon flow, a mixture of crystalline and glassy phases was obtained but the amount of the crystalline phase was much lower than that for air heat treatment. Also the crystalline phases formed in air and argon atmospheres were different. This preliminary study[7] points to a complex decomposition behaviour for impurity silicate phases which is dependent on the starting composition, temperature, heat-treatment time and gas atmosphere.

Based on this discussion it is therefore possible that, in the present study, for air-sintered specimens, the impurity silicate phase which forms in the bulk of zirconia ceramics below 1300°C may undergo a complex decomposition to a Na-rich glass which migrates to the external surface leaving behind, in the grain boundary network, an Y-rich silicate. It is worth mentioning here that the presence of Na_2O in the grain boundary network does not necessarily lead to its incorporation into the glassy phase.[8] Indeed Na_2O has been reported as a good flux for the reaction between SiO_2 and Y_2O_3.[8] Yttrium silicates have higher melting points than Na–Y-silicates.[9,10] Thus increasing the yttrium content of the silicate will raise its melting point. Consequently increased wetting of the grain boundary network between 1500 and 1600°C, as indicated by the XPS atomic ratios on the fracture surface, and a significant increase in the grain boundary resistivity may be due to melting of the Y-rich silicate. Above 1600°C, atomic ratios at the fractured surface as well as the grain boundary resistivity decrease, indicating that there is further dewetting of the grains, although it should be noted that the Si/Zr ratio for the fractured surface does not decrease to zero. A considerable amount of the impurity silicate phase appears to remain within the ceramic, presumably at triple points and other isolated pockets along the grain boundary surface area. This was reflected in the grain boundary resistivity at 1700°C, for air-sintered specimens, which was twice that for the argon-sintered discs.

The differences between air and Ar sintering have important ramifications for the successful processing of yttria–zirconia ceramics for industrial applications. It is evident from the data presented in this paper that the grain boundary network is never clean of impurity silicate phase under the sintering conditions used here. Consequently, as demonstrated by the impedance results, there will always be some contribution from the grain boundary to the total resistivity. By processing YSZ10V disks in an Ar environment, however, it was possible to purge the grain boundary network of most of the impurity silicate phase(s) by sintering at temperatures above 1500°C, as demonstrated by XPS and impedance measurements.

A final point worth discussing here is the implications of this work on various models considered before in the literature to describe the effect of grain boundary phases on the grain boundary resistivity in solid electrolytes. In a previous publication[11] the grain boundary behaviour in solid electrolytes was summarized in terms of two broad models. In the first model, segregation of impurities and components of the bulk phase were considered to form a continuous phase surrounding all the grains (Fig. 8(a)) and the grain boundary resistivity is the resistivity of a thin film of the glass phase. For this model, if chemically different glass phases are present at grain boundaries, then the activation energy may be expected to be different. Also, because of the different nature of the conduction processes involved, the activation energy for the lattice and grain boundary resistivities is expected to be significantly different. In the second model, a discontinuous grain boundary phase and some direct grain to grain contact was assumed (Fig.

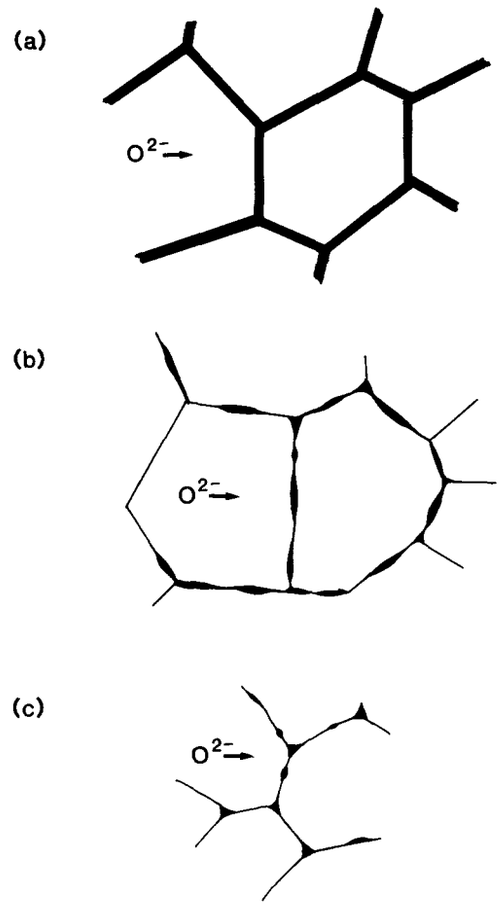

Fig. 8. Various models descriptive of the grain boundary region. (a) Continuous grain boundary phase completely surrounding all grains; (b) and (c) discontinuous grain boundary phase assuming incomplete but varying degree of wetting of the grains.

8(b) and (c)); the grain boundary surface area covered by the grain boundary phase depending on its amount, composition and wetting properties for given sintering conditions. Two limiting cases which take into account the relative contribution from two parallel paths for conduction, one through the contact between grains (intrinsic) and the second through the glass phase (extrinsic), were considered. The intrinsic region takes into account lattice mismatching, dislocations, defects, enhanced segregation of bulk components of the ceramic and second phase precipitation. For the second model, when the blocking effect of the glass phase is considerable, the activation energy for the grain boundary zone will be determined by the grain-to-grain contact region and will be independent of the nature of the glass phase. In this study, despite the different nature of the grain boundary phase for materials sintered in air and argon atmospheres, the activation energy for the grain boundary resistivity was about the same and was comparable with the activation energy for the lattice resistivity. This, along with XPS evidence and impedance behaviour as a function of the sintering temperature, strongly points to a discontinuous grain boundary phase model. Perfect wetting of grains may be possible in ceramics for certain types of grain boundary phase and for some sintering conditions. This, however, can not be considered as a universal model.

5 Conclusions

The sintering atmosphere used to sinter yttria–zirconia ceramics can have a marked effect on the type of impurity phase formed. It has been demonstrated, using XPS and impedance dispersion analysis, that sintering Y-FSZ in air creates a grain boundary impurity silicate phase which is resident in the grain boundary network at all sintering temperatures. Furthermore, the composition of the impurity silicate phase changes constantly with the sintering temperature. Firing in Ar, as previously reported by the present authors, produces entirely different results; the grain boundary network can be reasonably purged of the impurity silicate phase at temperatures in excess of 1500°C. Although the different behaviour reported in air- and Ar-sintered specimens is for a given powder, nevertheless a systematic study of materials sintered in different atmospheres may provide a good model system for examining the effects of liquid-phase assisted sintering. The results also point to a discontinuous grain boundary phase model and that wetting of grains does not occur under all sintering conditions. The high degree of correlation between the grain boundary resistivity and the XPS atomic ratios at the fracture surfaces as a function of the sintering temperature (air) provides complementary evidence that the impurity phase is more uniformly spread over grain boundaries at temperatures corresponding to the peaks in the atomic ratios.

Acknowledgements

The authors are thankful to K. Crane for assistance with some specimen preparation and Dr M. J. Bannister for reviewing this manuscript.

References

1. Badwal, S. P. S., Drennan, J., Hughes, A. E. & Sexton, B. A., A study of impurity phase segregation in fully stabilized yttria—zirconia. *Mater. Sci. Forum*, **34–36** (1988) 195–9.

2. Hughes, A. E. & Sexton, B. A., XPS study of an intergranular phase in yttria–zirconia. *J. Mater. Sci.*, **24** (1989) 1057–61.
3. Badwal, S. P. S. & Drennan, J., Yttria–zirconia: Effect of microstructure on conductivity. *J. Mater. Sci.*, **22** (1987) 3231–9.
4. Hughes, A. E., The identification of intergranular impurity phases in zirconia based ionic conductors. *Mater. Sci. Forum*, **34–36** (1988) 243–7.
5. Wagner, C. D. & Joshi, A., The Augur parameter, its utility and advantages: A review. *J. Electron. Spectrosc. Relat. Phenom.*, **47** (1988) 283–313.
6. Hughes, A. E. & Badwal, S. P. S., An XPS investigation of impurity glass in Y-TZP. *Mater. Sci. Forum*, **15** (1991) 261–7.
7. Smith, M. A. & Hughes, A. E., A NMR and XPS study of the crystallisation of sodium–yttrium silicate glasses, to be submitted.
8. Leslela, M. & Jyrkas, K., Effect of flux materials on the reaction of Y_2O_3 and SiO_2. *J. Amer. Ceram. Soc.*, **70** (1987) C160–C161.
9. Ito, J. & Johnson, H., Synthesis and study of yttrialite. *Amer. Miner.*, **53** (1968) 1940–52.
10. Cervantes, F., Marr, L. J. & Glasser, F. P., Compounds in the Na_2O–Y_2O_3–SiO_2 system. *Ceram. Int.*, **7** (1981) 43–7.
11. Badwal, S. P. S., Drennan, J. & Hughes, A. E., Segregation in oxygen-ion conducting solid electrolytes and its influence on electrical properties. In *Science of Ceramic Interfaces*, ed. J. Nowotny. Elsevier Science Publishing, London, 1991, pp. 227–85.